Int. J. Electrochem. Sci., 12 **(2017)** 4692 – 4701, doi: 10.20964/2017.06.89

International Journal of
ELECTROCHEMICAL
SCIENCE
www.electrochemsci.org

Hydrogen Evolution on Columnar Ni Thin Films Obtained by GLAD

Jelena Potočnik[1], *Maja Popović*[1], *Zlatko Rakočević*[1], *Svetlana Štrbac*[2,*]

[1] INS Vinča, Laboratory of Atomic Physics, University of Belgrade, Mike Alasa 12-14, 11001 Belgrade, Serbia
[2] ICTM-Institute of Electrochemistry, University of Belgrade, Njegoševa 12, 11000 Belgrade, Serbia
[*]E-mail: sstrbac@tmf.bg.ac.rs

Received: 20 March 2017 / *Accepted:* 18 April 2017 / *Published:* 12 May 2017

Nanostructured nickel thin films were deposited on glass using glancing angle deposition (GLAD) technique. Cross-sectional field emission scanning electron microscopy images have shown that obtained Ni thin films consist of vertical, tilted or zigzag nano-scaled columns, while X-ray diffraction have shown that (111) orientation prevailed. X-ray photoelectron spectroscopy revealed that apart from metallic nickel, NiO and $Ni(OH)_2$ were also present in lower amount. Cyclic voltammetry in alkaline solution has shown that hydrogen evolution reaction (HER) was significantly catalyzed on all columnar nanostructures compared to Ni(poly). This was ascribed to the high electroactive surface area (EASA) of porous nickel columns. EASAs for vertical, tilted and zigzag Ni thin layers were higher 32, 25.3, and 24.9 times, respectively, than their geommetric areas. Accordingly, Ni thin films with vertical columns have shown the highest activity for HER.

Keywords: nickel thin films, glancing angle deposition, hydrogen evolution reaction, alkaline solution

1. INTRODUCTION

Nickel is an attractive non-noble metal that has found wide application in electrocatalysis, particularly due to its high activity for hydrogen evolution reaction (HER) in alkaline solution [1-3]. Beside its metallic form, Ni can be utilized for construction of various types of electrodes either in the form of nanostructured thin films [4,5] or as a component of metallic alloys [6,7], which promote HER in alkaline solution.

Nanostructured Ni thin films or Ni based alloy films can be prepared using various techniques among which electrochemical [4,8-10] or electroless [11] deposition, and chemical [12,13] or physical vapor deposition [14] are most commonly used, including recently developed magnetron sputtering [15]. Physical vapor deposition where the incoming vapor atoms arrive on the substrate from an

oblique angle of incidence, and which is called glancing angle deposition (GLAD) technique is an emerging method for obtaining various metal columnar nanostructures [16]. The main property of this method is atomic shadowing mechanism, leading to preferential growth of existing nuclei and islands at the substrate surface. As these features grow, the shadowing effect is enhanced and promotes the formation of columnar structures, such as tilted and vertical posts, zigzag or helices. These specific structure of the thin films deposited by GLAD and their other physico-chemical properties, including their chemical composition and porosity are very important in determining their electrocatalytic activity for hydrogen production. Recently, a comprehensive study of the porosity of Ni thin films with vertical columns deposited using GLAD have been reported by the same group [17].

In this work, nickel thin films with different columnar structures were deposited on glass substrate using GLAD. Structural and chemical characterizations were performed by field emission scanning electron microscopy (FESEM), X-ray diffraction (XRD) and X-ray photoelectron spectroscopy (XPS). Cyclic voltammetry (CV) and HER studies were performed in alkaline solution.

2. EXPERIMENTAL

2.1. Deposition of nickel thin film

Nickel thin films were deposited on glass by electron beam evaporation, using home built glancing angle deposition equipment. Glass microscope slides (Thermo Scientific, Menzel-Glaser), cut into 1 x 0.5 cm^2 pieces were cleaned with ethanol, deionized water, and finaly in ozonizer before each deposition of nickel (99.98% purity, Onix-Met). Glass substrates were oriented in such way that the angle between the surface normal and the direction of the flux of evaporated nickel atoms was 65^0. Additionally, for vertical columns, the substrate was rotated with a suitable constant speed (~ 40 rpm) during the deposition. Ni thin films with vertical columns were deposited at a rate of ~ 2.5 nm/min to the thickness of 150±10 nm, while the ones with tilted and zigzag columns were deposited at a rate of ~ 3 nm/min to the thickness of 150±10 nm and 300±20 nm, respectively.

2.2. Structural and chemical characterization of the deposited nickel thin films

Structural characterization was performed by FESEM, Mira XMU TESCAN, using cross-sectional view in order to determine the thicknesses of Ni thin films, as well as the shape and the diameter of Ni columns. XRD analysis was performed using a Philips PW1050 with CuKa emission width λ= 0.15418 nm. Samples were recorded in 2θ range of 35^0–55^0. Chemical analysis was performed by XPS using SPECS with XP50M X-ray source and PHOIBOS 100/150 analyzer. Measurements were performed using a monochromatic Al Kα X-ray source (photon energy of 1486.74 eV), while e-flood gun was used to compensate the electron emission and prevent sample charging. High resolution spectra were taken in the fixed analyzer transmission mode with the analyzer pass energy of 20 eV.

2.3. Electrochemical measurements

Cyclic voltammetry was performed in deaerated 0.1 M KOH solution in a conventional three electrode cell, where mechanically polished polycrystalline Ni, Ni(poly), with the GA of 0.3 cm^2, and different Ni thin films deposited on glass, with the geometric area (GA) of 0.15 cm^2, were used as working electrodes. Electrodes consisting of Ni thin films deposited on glass were put in contact with the electrolyte using Pt wire threaded through the small hole (0.5 mm), which was drilled in the upper part of the electrode. That part stayed above the electrolyte, while the lower portion (0.5 cm x 0.3 cm) of such electrodes was immersed in the electrolyte facing the Luggin capillary close enough, so that the convinient geometry minimized the electrolyte resistance. Pt wire was used as counter, and Ag/AgCl, 3 M KCl as reference electrode. For HER measurements, the electrodes were additionally preconditioned at -1.1 V for 60 s.

2.4. Chemicals

Working solution was prepared from KOH (Merck), and Milli-pure water. In all CV experiments, KOH solutions were deoxygenated with 99.999 % N_2 (Messer). All measurements were performed at room temperature.

3. RESULTS AND DISCUSSION

3.1. Structural characterization of Ni thin films

Cross-sectional FESEM images and corresponding XRD diffractograms of Ni thin films with vertical, tilted and zigzag columnar structures are presented in Fig. 1. According to the obtained FESEM image, Fig. 1a, 150 nm thick Ni thin film consists of vertical columnar structures, with the average column diameter of 34 nm. XRD pattern, Fig. 1b, exhibits a well defined sharp peak at position of $2\theta = 44.75^0$ corresponding to (111) reflection of face centered cubic (FCC) Ni phase, and a very small peak at 52.11^0, which belongs to the reflection from (200) plane. SEM image for 150 nm thick Ni thin film, consisting of columns tilted for 47^o, and with the average column diameter of 26 nm is shown in Fig. 1c. XRD diffractogram, Fig. 1d, exhibits a broader peak centered at $2\theta = 44.62^o$, corresponding to (111) reflection of FCC Ni phase and a rather weak peak at $2\theta = 52.23^o$, corresponding to the reflection from (200) plane, showing again that the preferential orientation of Ni crystallites is (111). Cross-sectional FESEM image of 300 nm Ni thin film, Fig. 1e, shows zigzag columnar structure with the colum width of approx. 30 nm. While the bottom layer is tilted for 47^o, the top layer is tilted for 55^o. XRD diffractogram, Fig. 1f, shows a rather pronounced peak at $2\theta = 44.71^o$ corresponding to the (111) reflection from FCC Ni phase and a smaller peak at $2\theta = 52.10^o$, corresponding to the reflection from (200) plane. Based on the diffractograms for tilted and zigzag columns it can be seen that the (111) lines are wide, which indicates that the as-deposited Ni thin films have fine-grained structure. Low intensity of the diffraction line for Ni tilted columns also indicates

poor crystallinity of the deposited layer. According to the presented XRD results, it can be concluded that the preferential crystallite orientation of all obtained columnar nickel thin films is (111).

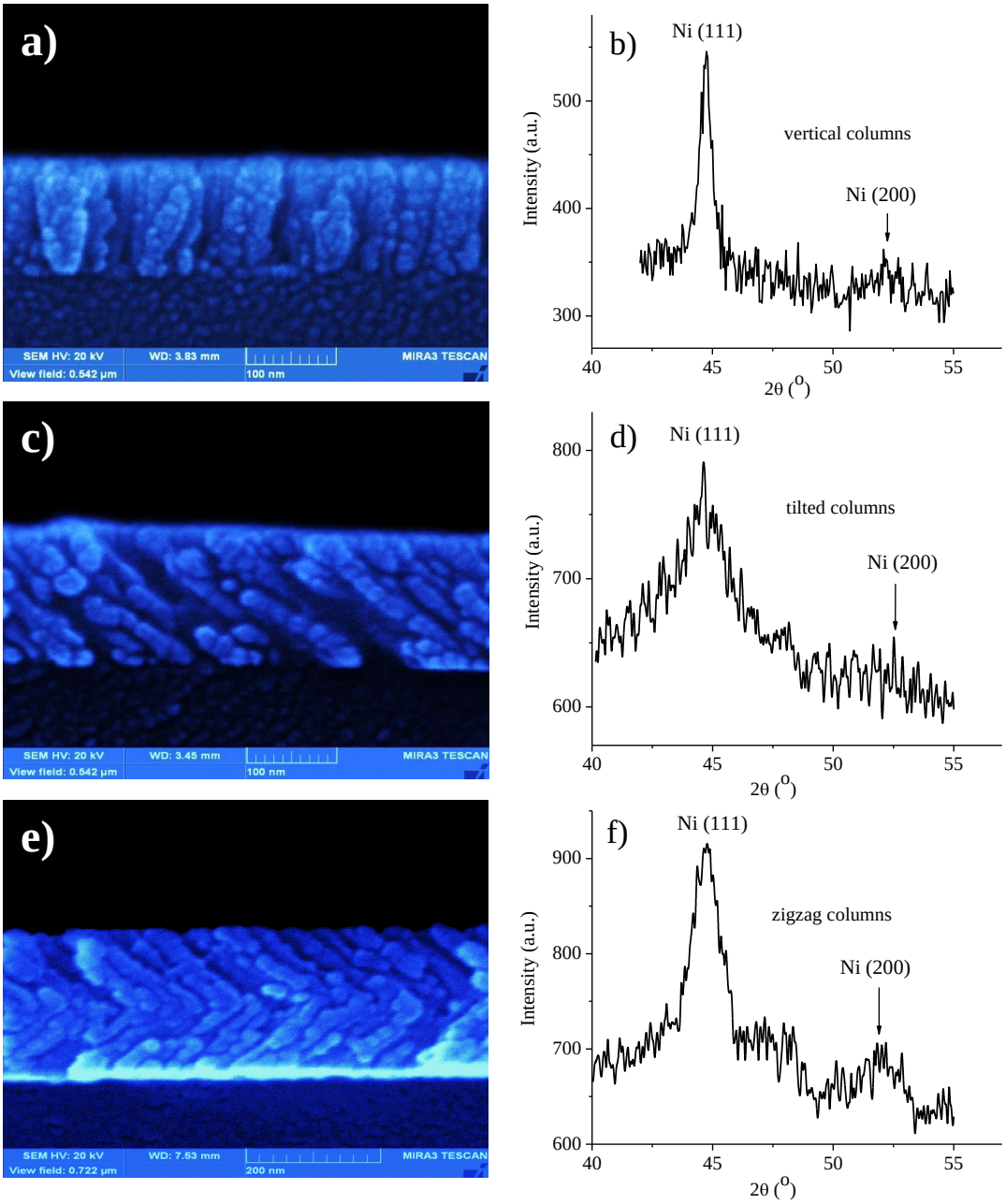

Figure 1. Cross-sectional SEM images (left column) and XRD diffractograms (right column) of different Ni thin films: a) and b) 150±10 nm thick vertical columns; c) and d) 150±10 nm thick tilted columns; e) and f) 300±20 nm thick zigzag columns.

XPS analysis has been performed to determine the elemental composition of obtained Ni thin films and to identify the chemical bonds. XPS composition analysis revealed that all Ni thin films consisted mainly of Ni (93.1 at.%), oxygen (4.2 at.%) and carbon (2.6 at.%) impurities, while Ni(poly) consisted of Ni (95.8 at.%), oxygen (1.2 at. %) and carbon (2.9 at.%). Since obtained high-resolution spectra of nickel and oxygen lines for various Ni thin films appeared identical for Ni $2p_{3/2}$ line, and

similar for O 1s line, only the data for 150 nm Ni thin film with tilted columns and for bare Ni(poly) are presented in Fig. 2. It can be seen that the Ni $2p_{3/2}$ line, Fig. 2a, is clearly asymmetric, which is typical for metallic samples. The main peak positioned at 852.2 eV, is shifted for 0.4 eV with respect to the one for Ni(poly), positioned at 852.6 eV Fig. 2c, which is in agreement with the literature data [18]).

Since the relative amount of oxygen is only few percent, contributions of either NiO or $Ni(OH)_2$, would be too low to be resolved from the much more intensive metallic nickel contribution. Therefore, high-resolution spectra of the O 1s line, were recorded in the range from 537 to 525 eV. O1s peak for 150 nm thick Ni thin film, which was fitted to four components is presented in Fig. 2b. Two dominant contributions at 529.8 eV and 531.2 eV can be attributed to NiO and $Ni(OH)_2$ [18], while smaller peaks at 532.8 eV is related to C-O-C group [19].

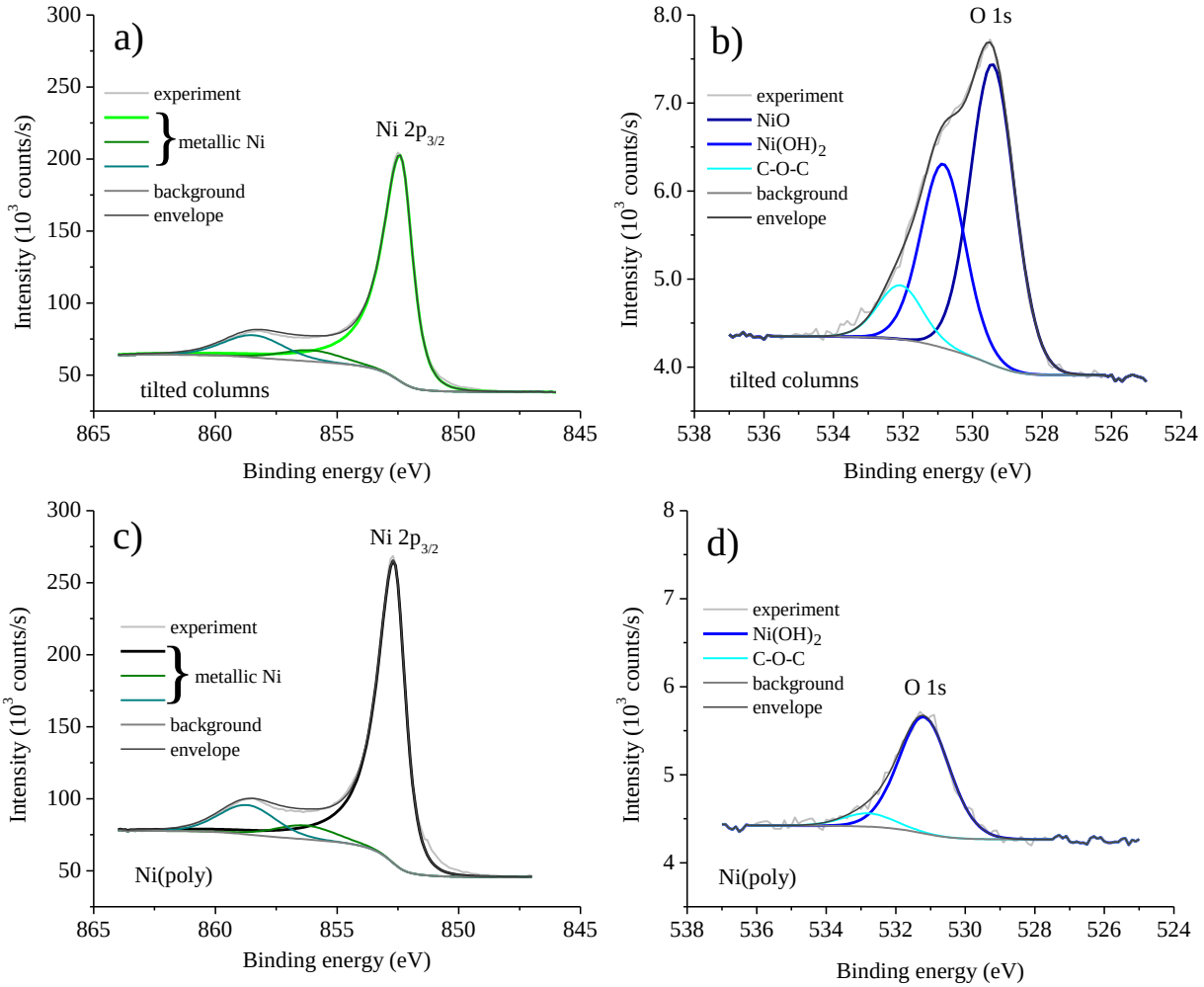

Figure 2. High-resolution XPS spectra Ni $2p_{3/2}$ (left column) and O1s (right column) photoelectron lines taken from: a) and b) 150±10 nm thick Ni thin film with tilted columns; c) and d) Ni(poly).

The amounts of NiO and $Ni(OH)_2$ relative contributions can be estimated from the oxygen content and the relative intensity of the O1s contribution attributed to NiO and $Ni(OH)_2$. According to the obtained fitting results, it can be seen that detected amount of NiO in deposited Ni film is 4.0 at.%, while the amount of $Ni(OH)_2$ in observed sample is equal to 2.6 at.%. When compared to O 1s line for bare Ni(poly), Fig. 2d, where only one component at 531.3 eV corresponding to $Ni(OH)_2$ is found, one can see that the presence of NiO is present only on the deposited Ni thin film. Similar results were also found for the other two samples and therefore will not be presented in this paper.

3.2. Cyclic voltammetry characterization of Ni thin film and hydrogen evolution reaction

Cyclic voltammograms of Ni thin films with vertical, tilted and zigzag columnar structures, recorded in 0.1 M KOH solution before and after conditioning for 60 s at -1.1 V, are shown in Fig. 3, together with CVs for Ni(poly) recorded for comparison under the same conditions.

Stabilized and reproducible CVs obtained after several cycles in the potential limits from -1.1 V to 0.65 V, Fig. 3a, show three distinct potential regions involving: cathodic hydrogen evolution, double layer, and well-defined anodic and cathodic peaks at higher potentials. The hydrogen evolution potential region show clearly that while HER on bare Ni(poly) occurs at lower potentials starting from -0.9, on all columnar Ni thin films it begins at more positive potentials. On Ni thin film with vertical columns the onset for HER at -0.75 V is mostly shifted compared to bare Ni(poly), thus demonstrating the highest activity. The anodic peaks at 0.58 V, 0.50 V and 0.52 V, for vertical, tilted and zigzag columnar Ni thin films, respectively, correspond to the formation of β-NiOOH oxide [3,20-22]. This oxide is reduced to β-$Ni(OH)_2$, showing cathodic peaks at 0.32 V, 0.38 V and 0.4 V, for vertical, tilted and zigzag columnar Ni thin films, respectively. Slight difference in oxide formation/reduction peak potentials reflects the difference in the orientation of the deposited different columnar Ni thin films [20]. Compared to bare Ni(poly) [23], it can be seen that for columnar Ni thin films, current densities for all CV features are significantly enhanced indicating a pronounced enlargement of the electrochemically active surface areas (EASA). By integrating oxide reduction peaks EASAs can be calculated taking into account that the reduction of β-NiOOH to β-$Ni(OH)_2$ involves one electron [20], and that the charge associated with monolayer formation is 257 $\mu C/cm^2$ [21]. Calculated charge for Ni(poly) of 500 $\mu C/cm^2$ means that its EASA is two times higher than the geommetric area (GA) due to the higher roughness with respect to an ideally flat Ni surface. The charges for vertical, tilted and zigzag thin layers are 8.26 mC/cm^2, 6.51 mC/cm^2 and 6.41 mC/cm^2, respectively, which gives the corresponding EASAs for 32, 25.3, and 24.9 times higher than GA. The origin of such enhanced EASAs of columnar Ni thin films can be explained by their porosity, which varies depending on the thickness and structure. Porosity was determined by the method shown in ref. [17], and for 150 nm thick vertical columnar Ni thin film, it was approx. 35%, while for tilted and zigzag thin films it was determined to be ~ 25% and ~47%, respectively. Cyclic voltammograms of Ni thin film with vertical columns recorded over the same larger potential region, after conditioning for 60 s at -1.1 V, are shown in Fig. 3b. The production of hydrogen was significantly enhanced by preconditioning at -1.1 V, which is ascribed to the high electroactive area of such porous electrode structure. During the

potential drive to the positive direction, the formation of α-$Ni(OH)_2$ in the first sweep and its subsequent irreversible phase transition to β-$Ni(OH)_2$ can be seen by the difference in the second sweep [21].

Fig. 4a shows CVs recorded within shorter potential limits from -1.1 V to -0.5 V, after preconditioning at -1.1 V for 60 sec. Current densities corresponding to both cathodic HER and anodic formation of α-$Ni(OH)_2$ on columnar Ni thin films are significantly enhanced with conditioning. They are also much higher in comparison with those for Ni(poly) surface recorded under the same conditions. Since columnar Ni thin films are porous, much higher amount of hydrogen is being adsorbed and subsequently evolved than on the Ni(poly) surface. If the current densities are normalized to the EASAs, Fig. 4b, the same trend is observed with respect to the activity for HER.

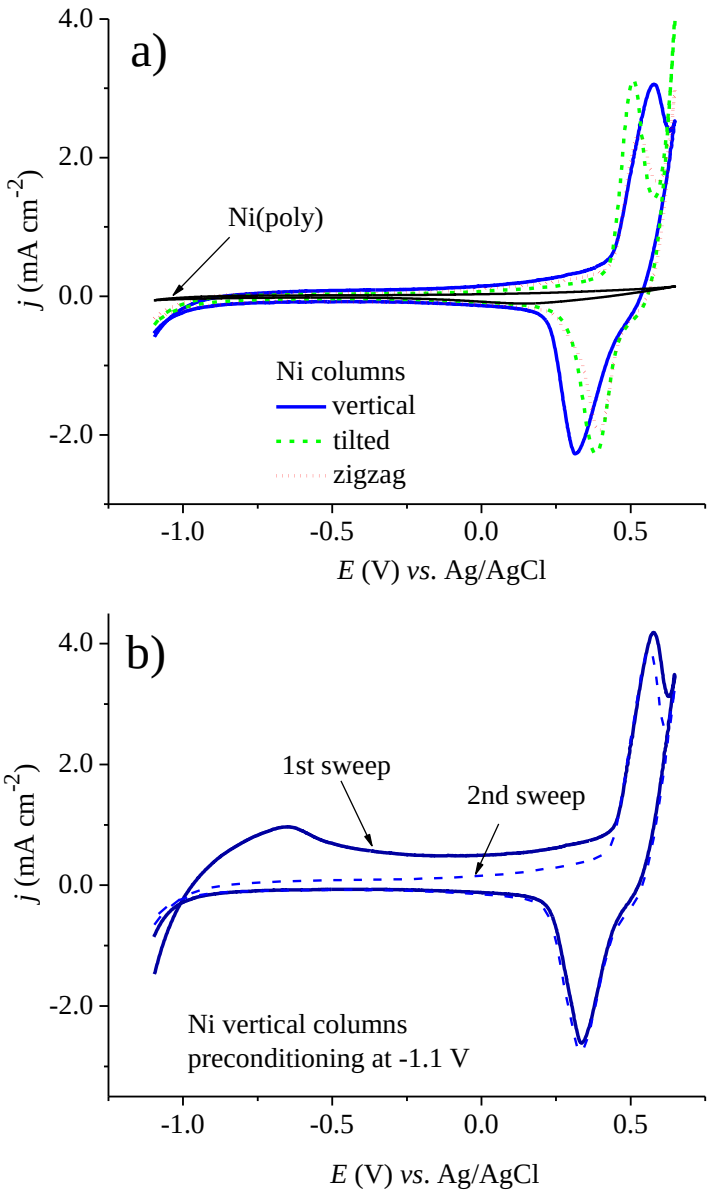

Figure 3. Cyclic voltammograms recorded in 0.1 M KOH: a) of different columnar Ni thin films; b) of Ni thin film with vertical columns, after preconditioning at -1.1 V for 60 s. Sweep rate 50 mV/s.

Presented results have demonstrated that columnar Ni thin films prepared by GLAD significantly catalyze HER, which opens up new possibilities for the preparation of catalysts with the enhanced EASA. Although all columnar Ni thin films have shown a significantly higher activity for hydrogen production, the one with vertical columns have shown the best performance, which is in accordance with their highest electrochemically active surface area. Future work will be focused on the search for the best substrate in order to obtain the most stable catalyst, as well as on the modification of Ni columnar thin films with the other metals in order to improve their catalytic activity for hydrogen production.

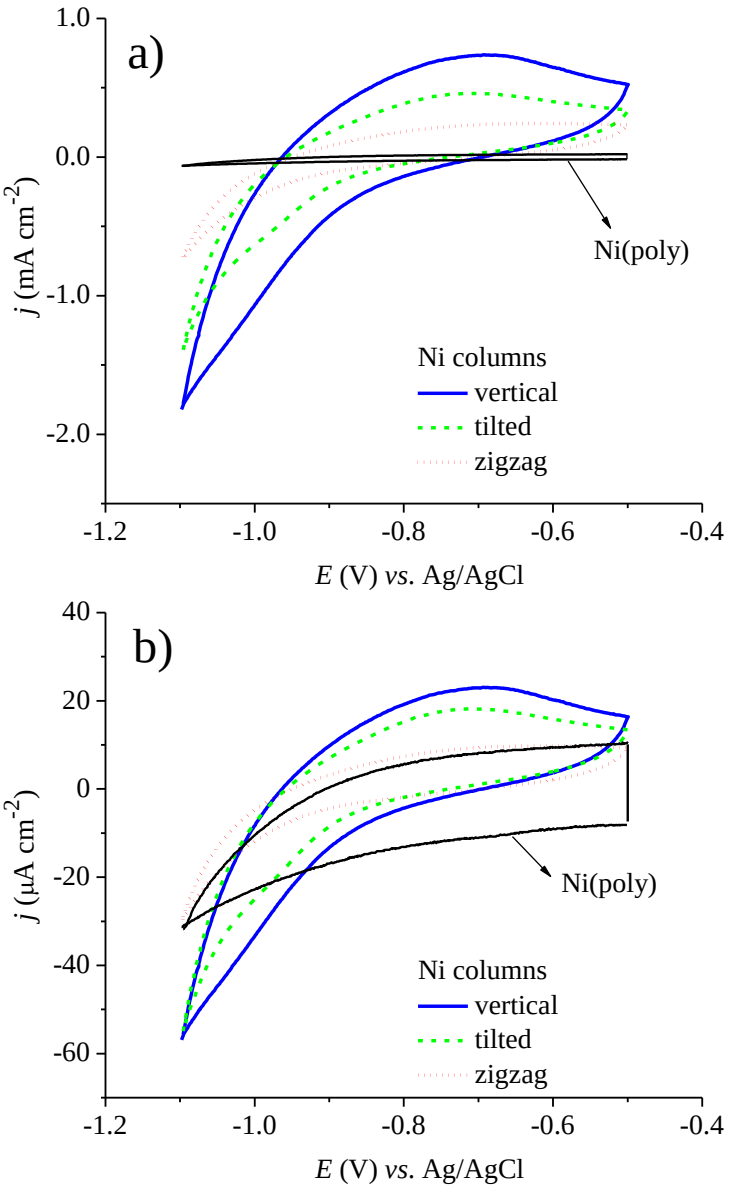

Figure 4. Cyclic voltammograms of different columnar Ni thin films recorded in 0.1 M KOH: a) of different columnar Ni thin films after preconditioning at -1.1 V for 60 s at a sweep rate of 50 mV/s; b) current densities normalized to EASA.

4. CONCLUSIONS

Nanostructured nickel thin films with the thicknesses of 150 nm or 300 nm, were deposited onto glass substrate using glancing angle deposition technique. The cross-sectional FESEM and XRD structural analyses have shown that Ni thin films consisted of vertical, tilted and zigzag columns, approx. 25 nm wide and mainly (111) oriented. XPS analysis revealed that all obtained columnar thin films consisted mainly of metallic Ni (> 90 at.%) and smaller amount of NiO and $Ni(OH)_2$. Hydrogen evolution reaction on Ni columnar thin films in alkaline solution is significantly catalyzed compared to bare Ni(poly), which was ascribed to the enlarged EASA due to their high porosity. Taking into account that the charge associated with Ni monolayer formation is 257 $\mu C/cm^2$, the charges obtained for vertical, tilted and zigzag thin layers, which were 8.26 mC/cm^2, 6.51 mC/cm^2 and 6.41 mC/cm^2, respectively, gave that the corresponding EASAs were 32, 25.3, and 24.9 times higher than their geommetric areas. Consequently, due to the highest EASA, Ni thin films with vertical columns have shown the best performance for HER.

ACKNOWLEDGEMENT

This work was financially supported by the Ministry of Science of the Republic of Serbia; project N^o 45005.

References

1. A. Lasia, A. Rami, *J. Electroanal. Chem.* 294 (1990) 123.
2. S.A.S. Machado, L.A. Avaca, *Electrochim. Acta*, 39 (1994) 1385.
3. D.S. Hall, C. Bock, B.R. MacDougall, *J. Electrochem. Soc.* 160 (2013) 235.
4. B.R. Cruz-Ortiz, M.A. Garcia-Lobato, E.R. Larios-Durán, E.M. Múzquiz-Ramos, J.C. Ballesteros Pacheco, *J. Electroanal. Chem.* 772 (2016) 38.
5. D. Pletcher, X. Li, S. Wang, *Int. J. Hydrogen Energy* 37 (2012) 7429.
6. W-F. Chen, K. Sasaki, C. Ma, A.I. Frenkel, N. Marinkovic, J.T. Muckerman, Y. Zhu, R.R. Adzic, *Angew. Chem. Int. Ed.* 51 (2012) 6131.
7. R. Solmaz, A. Doner, G. Kardas, *Electrochem. Commun.* 65 (2008) 1909.
8. M. Hasan, M. Jamal, K.M. Razeeb, *Electrochim. Acta*, 60 (2012) 193.
9. L. Gu,Y. Wang, R. Lu, L. Guan, X. Peng, J. Sha, *J. Mater. Chem. A*, 2 (2014) 7161.
10. Y. Yu, L. Sun, H. Ge, G. Wei, L. Jiang, *Int. J. Electrochem. Sci.* 12 (2017) 485.
11. X. Zhao, F. Muench, S. Schaefer, J. Brötz, M. Duerrschnabel, L. Molina-Luna, H.J. Kleebe, S. Liu, J. Tan, W. Ensinger, *Electrochem. Commun.* 65 (2016) 39.
12. J. Jiang, J. Liu, W. Zhou, J. Zhu, X. Huang, X. Qi, H. Zhang, T. Yu, *Energy Environ. Sci.* 4 (2011) 5000.
13. K.T. Chan, J.J. Kan, C. Doran, L. Ouyang, D.J. Smith, E.E. Fullerton, *Philos. Mag.* 92 (2012) 2173.
14. S. Xu, C. Wang, S.A. Francis, R.T. Tucker, J.B. Sorge, R.B. Moghaddam, M.J. Brett, S.H. Bergens, *Electrochim. Acta*, 151 (2015) 537.
15. X. Zhang, J. Hampshire, K. Cooke, X. Li, D. Pletcher, S. Wright, K. Hyde, *Int. J. Hydrogen Energy* 40 (2015) 2452.
16. M.M. Hawkeye, M.T. Taschuk, M.J. Brett, Glancing Angle Deposition of Thin Films: Engineering the Nanoscale, John Wiley & Sons, 2014.

17. J. Potočnik, M. Nenadović, N. Bundaleski, M. Popović, Z. Rakočević, *Opt. Mater.* 62 (2016) 146.
18. M.C. Biesinger, B.P. Payne, L.W.M. Lau, A. Gerson, R.S.C. Smart, *Surf. Interface Anal.* 41 (2009) 324.
19. M.C. Biesinger, B.P. Payne, A.P. Grosvenor, L.W.M. Lau, A.R. Gerson, R.St.C. Smart, *Appl. Surf. Sci.* 257 (2011) 2717.
20. B. Beden, D. Floner, J.M. Leger, C. Lamy, *Surf. Sci.* 162 (1985) 822.
21. M. Alsabet, M. Grdeń, G. Jerkiewicz, *Electrocatal.* 6 (2015) 60.
22. M. Vuković, *J. Appl. Electrochem.* 24 (1994) 878.
23. A.Mazzi N.Bazzanella, M.Orlandi, R.Edla, N.Patel, R.Fernandes, A.Miotello, *Mater. Sci. Semicond. Process.* 42 (2016) 155.